

Nickel(II) and nickel(0) complexes of bis(diisopropylphosphino)amine: Synthesis, structure, and electrochemical activity

Diane A. Dickie,^a Brittany E. Chacon,^b Alibek Issabekov^c, Kevin Lam^{*c} and Richard A. Kemp^{*a,b}

^a Department of Chemistry and Chemical Biology, University of New Mexico, Albuquerque, NM, USA, 87111.

^b Advanced Materials Laboratory, Sandia National Laboratories, Albuquerque, NM, USA, 87106.

^c Department of Chemistry, School of Science and Technology, Nazarbayev University, Astana, Kazakhstan, 010000.

Corresponding authors. E-mail: kevin.lam@nu.edu.kz; rakemp@unm.edu.

ABSTRACT

In its neutral state, bis(diisopropylphosphino)amine **HL** reacts in equimolar amounts with the nickel halides NiCl₂•6H₂O, NiBr₂, and NiI₂ in ethanol solutions to give the air- and moisture-stable P,P-chelated complexes (**HL**)NiX₂ (X = Cl, Br, I). Under similar conditions, complexes of the form [(**HL**)₂Ni]X₂ (X = BF₄, NO₃, ClO₄) were prepared from 2:1 ligand-metal ratios of Ni(BF₄)₂•6H₂O, Ni(NO₃)₂•6H₂O, or Ni(ClO₄)₂•6H₂O. Deprotonation of the ligand with NaNH₂ followed by reaction with NiI₂ gives **L**₂Ni when performed in Et₂O, but leads to the co-crystal **L**₂Ni•2[NCCHC(Me)NH₂] when the solvent is acetonitrile. In addition to these Ni²⁺ compounds, the Ni⁰ complex (**HL**)Ni can be prepared from a toluene solution of Ni(cod)₂. Each complex has been characterized by a combination of IR and multi-nuclear NMR spectroscopies, as well as single-crystal X-ray diffraction. Electrochemical studies of the complexes revealed irreversible decomposition of the (**HL**)NiX₂ (X = Cl, Br, I) series, but electrocatalytic CO₂ reduction by the [(**HL**)₂Ni]X₂ (X = BF₄, NO₃, ClO₄) compounds.

1. INTRODUCTION

Nickel complexes in which the metal is bound to at least two phosphorus atoms are a very versatile class of molecules. They have been used as stoichiometric reagents for hydrosilation,[1] to form nickelaioxetanes as models for catalytic oxidation processes,[2] and to make mixed-metal compounds to model heterogeneous clusters[3]. They have been used as active catalysts, pre-catalysts, or catalytic model compounds for photoelectrochemical water splitting,[4] ethylene oligomerization and polymerization,[5] functionalization of unsaturated hydrocarbons,[6] cross-coupling reactions, [7] and other processes.[8] Of most interest to us, they are used for the activation and conversion of CO₂,[9] an area of growing concern both academically and industrially.[10]

In many cases, the active nickel species is generated by combining the metal and phosphine ligand *in situ*, with little or no characterization of the resulting complex. Nevertheless, more than 2300 mononuclear NiP₂ complexes have been characterized by single-crystal X-ray diffraction.[11] Of these, approximately 100 contain bidentate ligands with a single-atom bridge between the phosphorus centers. With a few exceptions, the bridging atom is split roughly equally between N and C. A closer examination of these structures reveals a striking difference between these two groups. While most of the carbon bridges are simple methylene (–CH₂–) fragments, the vast majority of the nitrogen bridges are tertiary amines, with alkyl, aryl, or other groups as the third substituent. Only four complexes contain an unsubstituted nitrogen atom. Of those four complexes, three are based on the neutral ligands HN[P(*t*-Bu)₂PMe(*t*-Bu)][12] or HN(PPh₂)₂,[13], while the fourth uses the latter in its anionic, deprotonated form [N(PPh₂)₂]⁻. We

have previously shown that this anionic ligand will react with CO₂ in rather unexpected ways when bound to either Mg,[14] Ca or Sr,[15] or Zn.[16] When the phenyl groups are replaced by isopropyl groups, we have found that the reactivity is often more straightforward. The anion {N[P(*i*-Pr)₂]₂}⁻ will chelate main group elements through the phosphorus atoms, and the resulting Zn[16], Sn,[17] or In[18] complexes will insert CO₂ into the M-P bonds. Each of these complexes, however, is unstable in the presence of moisture, a serious drawback to any future, large-scale operation for CO₂ capture and recycle/conversion. We hypothesized that if the ligand were kept in its neutral form HN[P(*i*-Pr)₂]₂, the resulting complexes would be more likely to tolerate moisture and other protic environments. As well, with an eye towards a possible future capture and conversion process, Ni is fortunately an earth abundant metal, as are our previously-used Zn and Sn metals.

2. Experimental

2.1 General Considerations

All manipulations were carried out in an argon-filled glovebox or by using standard Schlenk techniques unless otherwise noted. The ligand bis(diisopropylphosphino)amine **HL** was prepared according to literature procedures.[19] Anhydrous solvents were stored in the glovebox over 4 Å molecular sieves prior to use. ¹H and ¹³C{¹H} spectra were referenced to residual solvent downfield of TMS. ³¹P{¹H}, ¹¹B{¹H}, and ¹⁹F{¹H} spectra were referenced to external 85% H₃PO₄, BF₃•Et₂O, and C₆F₆, respectively. Due to low solubility, ¹³C{¹H} NMR was not obtained for most compounds. IR spectra were recorded as mineral oil mulls on KBr windows. Elemental analyses were performed by ALS Global (Tucson, AZ) or on a Perkin Elmer 2400 Series II CHNS/O Analyzer. Single-crystal X-ray diffraction studies were performed on a Bruker Kappa Apex II CCD diffractometer. Crystals were coated in Paratone-N oil and mounted on a

MiTeGen MicroLoopTM. The Bruker Apex3 software suite[20] was used for data collection, structure solution and refinement. Crystal data are summarized in Table 1.

Electrochemical measurements were carried out using an Autolab 302N potentiostat interfaced through Nova 2.0 software to a personal computer. Electrochemical measurements were performed using 0.1M [Bu₄NPF₆]/THF electrolyte solutions from solvent that had been purified by passing through an alumina-based purification system. Diamond-polished glassy carbon electrodes of 3mm diameter were employed for cyclic voltammetry (CV) scans. CV data were evaluated using standard diagnostic criteria for diffusion control and for chemical and electrochemical reversibility. The experimental reference electrode was a silver wire coated with anodically deposited silver chloride and separated from the working solution by a fine glass frit. The electrochemical potentials in this paper are referenced to ferrocene/ferrocenium couple, as recommended elsewhere.[21] The ferrocene potential was obtained by its addition to the analyte solution[22] at an appropriate time in the experiment.

2.2 Synthesis of (HL)NiCl₂ (**1**)

NiCl₂·6H₂O (1.0 mmol) was dissolved in 10 mL EtOH and warmed to 50 °C in air to get a yellow solution. A colorless solution of **HL** (0.25 g, 1.0 mmol) in 5 mL EtOH was then added, and the solution immediately turned bright red. The solution was allowed to cool slowly to room temperature and was then further cooled to 4 °C. After 24 h, the supernatant was decanted from red, X-ray quality single crystals. Yield = 0.23 g (61%), mp = >200 °C. IR ν 3202 (br, N-H) cm⁻¹. ¹H{³¹P} NMR (300 MHz, CD₂Cl₂): δ 1.33 (d, ³J_{HH} = 7.2 Hz, 12H, CH₃), 1.57 (d, ³J_{HH} = 7.2 Hz, 12H, CH₃), 2.41 (sept, ³J_{HH} = 7.2 Hz, 4H, CH), 3.07 (s, 1H, NH) ppm. ³¹P{¹H} NMR (121

MHz, CD₂Cl₂): δ 63.9 ppm. Anal Calcd. for C₁₂H₂₉Cl₂NNiP₂: C, 38.04; H, 7.71; N, 3.70. Found: C, 38.06; H, 8.31; N, 3.71.

2.3 Synthesis of (HL)NiBr₂ (2)

NiBr₂ (0.22 g, 1.0 mmol) was partially dissolved in 10 mL EtOH and warmed 50 °C in air to get a peach-colored suspension. A colorless solution of **HL** (0.25 g, 1.0 mmol) in 5 mL EtOH was then added, and the mixture immediately turned bright red. The heterogeneous mixture was held at 50 °C for two hours, and was then allowed to cool slowly to room temperature. After 24 hrs, the supernatant was decanted from the red-orange powder. Yield = 0.32 g (68 %), mp = >200 °C. IR ν 3186 (br, N-H) cm⁻¹. ¹H{³¹P} NMR (300 MHz, CD₂Cl₂): δ 1.34 (d, ³J_{HH} = 7 Hz, 12H, CH₃), 1.59 (d, ³J_{HH} = 7 Hz, 12H, CH₃), 2.47 (sept, ³J_{HH} = 7 Hz, 4H, CH), 3.11 (br s, 1H, NH) ppm. ³¹P{¹H} NMR (121 MHz, CD₂Cl₂): δ 71.9 ppm. Anal Calcd. for C₁₂H₂₉Br₂NNiP₂: C, 30.81; H, 6.25; N, 2.99. Found: C, 30.03; H, 6.43; N, 2.93. X-ray quality single crystals were grown by slow evaporation of the NMR solution.

2.4 Synthesis of (HL)NiI₂ (3)

NiI₂ (0.31 g, 1.0 mmol) was combined with 10 mL EtOH and warmed 50 °C in air. A colorless solution of **HL** (0.25 g, 1.0 mmol) in 5 mL EtOH was then added, and the mixture immediately turned dark red. The heterogeneous mixtures was held at 50 °C for five hours, and was then allowed to cool slowly to room temperature. After 24 hrs, the supernatant was decanted from the purple-red powder. Yield = 0.39 g (69%), mp = >200 °C. IR ν 3192 (w, N-H) cm⁻¹. ¹H{³¹P} NMR (300 MHz, CD₂Cl₂): δ 1.34 (d, ³J_{HH} = 7.2 Hz, 12H, CH₃), 1.58 (d, ³J_{HH} = 7.2 Hz, 12H, CH₃), 2.52 (sept, ³J_{HH} = 7.2 Hz, 4 H, CH), 3.27 (br s, 1H, NH) ppm. ³¹P{¹H} NMR (121 MHz, CD₂Cl₂) δ 84.1 ppm. Anal Calcd. for C₁₂H₂₉I₂NNiP₂: C, 25.65; H, 5.20; N, 2.49.

Found: C, 25.02; H, 5.40; N, 2.45. X-ray quality single crystals were grown by slow evaporation of the NMR solution.

2.5 Synthesis of $[(HL)_2Ni](ClO_4)_2$ (**4**)

$Ni(ClO_4)_2 \cdot 6H_2O$ (0.37 g, 1.0 mmol) was dissolved in 10 mL EtOH and warmed to 50 °C in air to get a pale green solution. A colorless solution of **HL** (0.50 g, 2.0 mmol) in 10 mL EtOH was then added, and solution immediately turned bright yellow. The solution was allowed to cool slowly to room temperature and was then further cooled to 4 °C. After 24 h, the supernatant was decanted from yellow, X-ray quality single crystals. Yield = 0.45 g (59%), mp = >200 °C. IR ν 3150 (br, N-H) cm^{-1} . $^1H\{^{31}P\}$ NMR (300 MHz, CD_2Cl_2): δ 1.37 (d, $^3J_{HH} = 7$ Hz, 24H, CH_3), 1.46 (d, $^3J_{HH} = 7$ Hz, 24H, CH_3), 2.44 (sept, $^3J_{HH} = 7$ Hz, 8H, CH), 6.01 (s, 2H, NH). $^{31}P\{^1H\}$ NMR (121 MHz, CD_2Cl_2): δ 70.9 ppm. Anal Calcd. for $C_{24}H_{58}Cl_2N_2NiO_8P_4$: C, 38.12; H, 7.73; N, 3.70. Found: C, 37.14; H, 8.03; N, 3.65.

2.6 Synthesis of $[(HL)_2Ni](NO_3)_2$ (**5**)

Same as **4**, beginning with $Ni(NO_3)_2 \cdot 6H_2O$ (0.29 g, 1.0 mmol). Yield = 0.48 g (70%), mp = 191-193 °C. IR ν 2569 (m, N-H) cm^{-1} . $^1H\{^{31}P\}$ NMR (300 MHz, CD_2Cl_2): δ 1.35 (d, $^3J_{HH} = 7$ Hz, 24H, CH_3), 1.46 (d, $^3J_{HH} = 7$ Hz, 24H, CH_3), 2.43 (sept, $^3J_{HH} = 7$ Hz, 8H, CH), 8.36 (s, 2H, NH) ppm. $^{31}P\{^1H\}$ NMR (121 MHz, CD_2Cl_2): δ 67.4 ppm. Anal Calcd. for $C_{24}H_{58}N_4NiO_6P_4$: C, 42.31; H, 8.58; N, 8.22. Found: C, 42.29; H, 8.89; N, 8.20.

2.7 Synthesis of $[(HL)_2Ni](BF_4)_2$ (**6**)

Same as **4**, beginning with $Ni(BF_4)_2 \cdot 6H_2O$ (0.34 g, 1.0 mmol). Yield = 0.34 g (47 %), mp = >200 °C. IR ν 3245 (s, N-H) cm^{-1} . $^1H\{^{31}P\}$ NMR (300 MHz, C_6D_6): δ 1.36 (d, $^3J_{HH} = 7$ Hz,

24H, CH₃), 1.47 (d, ³J_{HH} = 7 Hz, 24H, CH₃), 2.43 (sept, ³J_{HH} = 7 Hz, 8H, CH), 5.75 (s, 2H, NH). ³¹P{¹H} NMR (121 MHz, CD₂Cl₂): δ 70.7 ppm. ¹⁹F{¹H} NMR (282 MHz, CD₂Cl₂) δ -149.9 ppm. ¹¹B{¹H} NMR (96 MHz, CD₂Cl₂) δ 0.90 ppm. Anal Calcd. for C₂₄H₅₈B₂F₈N₂NiP₄: C, 39.44; H, 8.00; N, 3.83. Found: C, 39.60; H, 8.22; N, 3.79.

2.8 Synthesis of L₂Ni (7)

NaNH₂ (0.08 g, 2.0 mmol) was added to a colorless solution of **HL** (0.50 g, 2.0 mmol) in 15 mL anhydrous Et₂O. The mixture was allowed to stir at rt for 1.5 h, and then NiI₂ (0.31 g, 1.0 mmol) was added. After stirring for 24 h at rt, NaI was removed by filtration and the volume of the orange solution was reduced under vacuum to ca. 4 mL. Upon cooling to -25 °C, orange crystals were isolated. Yield = 0.47 g (85 %), mp = dec >145 °C. ¹H{³¹P} NMR (300 MHz, C₆D₆): δ 1.15 (d, ³J_{HH} = 7 Hz, 24H, CH₃), 1.41 (d, ³J_{HH} = 7 Hz, 24H, CH₃), 1.88 (sept, ³J_{HH} = 7 Hz, 8H, CH) ppm. ¹³C{¹H} NMR (75 MHz, C₆D₆) δ 16.7 (s, CH₃), 19.0 (s, CH₃), 30.9 (vt, CH) ppm. ³¹P{¹H} NMR (121 MHz, C₆D₆) δ 24.3 ppm. Anal Calcd. for C₂₄H₅₆N₂NiP₄: C, 51.91; H, 10.17; N, 5.04. Found: C, 52.64; H, 10.62; N, 5.28.

2.9 Synthesis of L₂Ni•2[NCCHC(Me)NH₂] (7a)

NaNH₂ (0.08 g, 2.0 mmol) was added to a colorless solution of **HL** (0.50 g, 2.0 mmol) in 15 mL anhydrous MeCN. The mixture was allowed to stir at rt for 1h, and then NiI₂ (0.31 g, 1.0 mmol) was added. Over the course of 3.5 h, an orange solution with a yellow-orange ppt formed. Volatiles were removed under vacuum, and the residue was suspended in CH₂Cl₂. Insoluble NaI₂ was separated by filtration, and then the solvent was removed under vacuum to give a yellow-orange powder. Yield = 0.56 g (78 %), mp = 93-94 °C. ¹H{³¹P} NMR (300 MHz, CD₂Cl₂): δ 1.13 (d, ³J_{HH} = 7 Hz, 24H, CH₃), 1.38 (d, ³J_{HH} = 7 Hz, 24H, CH₃), 1.94 (sept, ³J_{HH} = 7

Hz, 8H, *CH*), 2.09 (s, 6H, *CCH*₃), 3.77 (s, 4H, *NH*₂), 4.09 (s, 2H, *CCH*) ppm. ¹³C{¹H} NMR (75 MHz, CD₂Cl₂) δ 16.9 (s, CH₃), 19.3 (s, CH₃), 19.9 (s, CCH₃), 20.4 (s, CCH₃), 31.0 (vt, PCH), 62.0 (s, CH), 63.7 (s, CH), 119.9 (s, CN), 122.0 (s, CN), 161.9 (s, CCH₃), 162.4 (s, CCH₃) ppm. ³¹P{¹H} NMR (121 MHz) δ 24.9 ppm (C₆D₆); 29.1 ppm (CD₂Cl₂). Anal Calcd. for C₃₂H₆₈N₆NiP₄: C, 53.42; H, 9.53; N, 11.68. Found: C, 53.42; H, 9.79; N, 11.82. X-ray quality single crystals were grown from a concentrated CH₂Cl₂ solution.

2.10 Synthesis of (HL)₂Ni (**8**)

Ni(cod)₂ (0.28 g, 1.0 mmol) was dissolved in 10 mL toluene to give a yellow solution. HL (0.50 g, 2.0 mmol) was added and the solution was allowed to stir at rt for 2 h. Volatiles were removed under vacuum and the residue was dissolved in 1 mL pentane and cooled to -25 °C. After 24 hrs, the dark supernatant was decanted from yellow block-like crystals. Yield = 0.31 g (56%), mp = dec >175 °C. ¹H{³¹P} NMR (300 MHz, C₆D₆): δ 1.21 (d, ³J_{HH} = 7.2 Hz, 12H, *CH*₃), 1.23 (d, ³J_{HH} = 7.2 Hz, 12H, *CH*₃), 1.72 (s, 1H, *NH*), 1.90 (sept, ³J_{HH} = 7.2 Hz, 4H, *CH*) ppm. ¹³C{¹H} NMR (75 MHz, C₆D₆) δ 18.4 (s, CH₃), 19.1 (s, CH₃), 29.2 (vt, CH) ppm. ³¹P{¹H} NMR (121 MHz, C₆D₆) δ 97.9 ppm. IR (Nujol mull) ν 3323 (NH) cm⁻¹. Anal Calcd. for C₂₄H₅₈N₂NiP₄: C, 51.72; H, 10.49; N, 5.03. Found: C, 52.02; H, 10.56; N, 4.91.

Table 1. Crystallographic data for compounds 1-8.

	1	2	3	4	5	6	7	7a	8
Chemical formula	$C_{12}H_{29}Cl_2NNiP_2$	$C_{12}H_{29}Br_2NNiP_2$	$C_{12}H_{29}I_2NNiP_2$	$C_{24}H_{58}B_2F_8N_2NiP_4$	$C_{24}H_{58}N_4NiO_6P_4$	$C_{24}H_{58}Cl_2N_2NiO_8P_4$	$C_{24}H_5N_2NiP_4$	$C_{32}H_{68}N_6NiP_4$	$C_{24}H_{58}N_2NiP_4$
Formula weight	378.91	467.83	561.81	730.93	681.33	756.21	555.29	719.51	557.31
space group	$P2_1/c$	$P2_1/c$	$P2_1/n$	$Pbca$	$Pbca$	$Pbca$	$Pbca$	$Pbca$	$P-1$
a (Å)	14.2872(4)	14.760(3)	8.2480(2)	14.7820(5)	14.6971(3)	14.8131(5)	14.9194(5)	11.1122(7)	9.8762(7)
b (Å)	9.8464(3)	9.7000(17)	21.7270(7)	15.0262(4)	14.9693(3)	13.7858(5)	11.5824(3)	18.8293(11)	10.4809(7)
c (Å)	14.2512(4)	14.658(3)	10.6538(3)	16.0322(5)	15.2423(3)	17.6853(7)	17.2569(5)	38.577(2)	17.0194(12)
α (°)									78.782(2)
β (°)	118.8760(10)	119.617(3)	92.537(2)						74.775(2)
γ (°)									64.898(2)
V (Å ³)	1755.56(9)	1824.4(6)	1907.34(9)	3561.03(19)	3353.39(12)	3611.5(2)	2982.03(15)	8071.7(8)	1532.34(19)
Z	4	4	4	4	4	4	4	8	2
D_{calcd} (g cm ⁻³)	1.434	1.703	1.956	1.363	1.350	1.391	1.237	1.184	1.208
μ (mm ⁻¹)	1.577	5.605	4.409	0.785	0.811	0.906	0.880	0.668	0.856
R ($I > 2\sigma I$)	0.0286	0.0384	0.0266	0.0520	0.0283	0.0443	0.0264	0.0413	0.0294
R_w ($I > 2\sigma I$)	0.0589	0.0613	0.0448	0.1325	0.0700	0.1015	0.0622	0.0826	0.0644

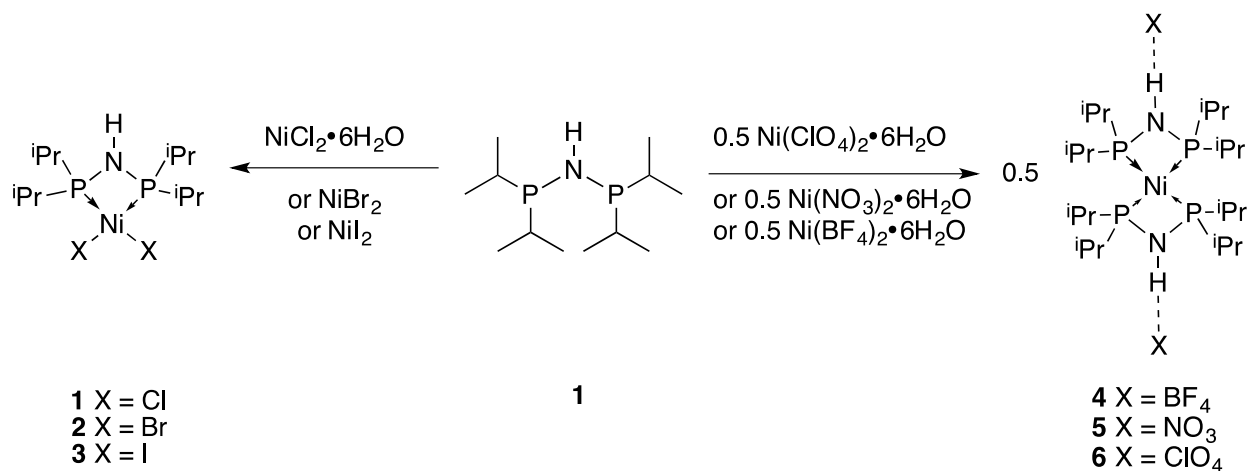
3. RESULTS AND DISCUSSION

3.1 Synthesis and structure

To the best of our knowledge, there is only one previous example in which $\text{HN}[\text{P}(i\text{-Pr})_2]_2$ (**HL**) has been directly used as a neutral ligand rather than as an anion. In that case, **HL** coordinates in a monodentate manner to $\text{B}(\text{C}_6\text{F}_5)_3$ through one of its P atoms and the amine H atom shifts to the other P.[23] In addition, a Pt complex of **HL** is claimed in the patent literature,[24] and Woollins and co-workers have reported the low-yield formation of a ruthenium complex containing **HL**, but in that case it formed via an *in situ* reduction of the disulfide $\text{HN}[\text{P}(=\text{S})(i\text{-Pr})_2]_2$ rather than directly from **HL**. [25]

The nickel(II) halides NiCl_2 , NiBr_2 and NiI_2 react with $\text{HN}[\text{P}(i\text{-Pr})_2]_2$ (**HL**) in warm ethanol to give complexes with the general formula $(\text{HL})\text{NiX}_2$. These red complexes **1** ($\text{X} = \text{Cl}$), **2** ($\text{X} = \text{Br}$), and **3** ($\text{X} = \text{I}$) can be handled and stored in air and do not appear to be sensitive to water. In fact, while **1** was initially prepared from anhydrous NiCl_2 , there was found to be no advantage to using that starting material over the much less expensive and more soluble $\text{NiCl}_2 \cdot 6\text{H}_2\text{O}$, and so the hexahydrate was used for all subsequent preparations (Scheme 1). Once formed, the complexes **1-3** were found to have relatively poor solubilities in most solvents and as such we were unable to obtain solution-phase $^{13}\text{C}\{^1\text{H}\}$ NMR data, but the $^1\text{H}\{^{31}\text{P}\}$ and $^{31}\text{P}\{^1\text{H}\}$ spectra were recorded in CD_2Cl_2 . The $^1\text{H}\{^{31}\text{P}\}$ spectra were shifted significantly downfield relative to the free ligand with the *CH* septet appearing at 2.41, 2.47 and 2.52 ppm for **1**, **2** and **3**, respectively, and the pair of *CH*₃ doublets at 1.33/1.57, 1.34/1.59, and 1.34/1.58 ppm. The *NH* proton was observed as a broad singlet at 3.07, 3.11 and 3.27 ppm for the three complexes, and the corresponding N-H IR stretches were found at 3202, 3186 and 3192 cm^{-1} . In contrast to the similar chemical shifts of the ^1H NMR signals, the $^{31}\text{P}\{^1\text{H}\}$ spectra of **1-3** were more varied. The

chloride derivate **1** appeared at 63.9 ppm, upfield from the free ligand at 69.1 ppm. The bromide **2** and iodide **3**, however, were shifted downfield, to 71.9 and 84.1, respectively.



Scheme 1. Synthesis of nickel complexes (HL)NiX₂ **1-3** and [(HL)₂Ni]X₂ **4-6**.

The spectroscopic data strongly indicated that **HL** binds to the nickel halides as a P,P-chelating ligand with the NH bond intact, in contrast to the monodentate coordination with NH/PH tautomerization seen upon reaction with B(C₆F₅)₃.^[23] To confirm the exact nature of the complexes **1-3**, they were examined by single crystal X-ray diffraction. Suitable crystals of **1** were obtained directly from the reaction mixture upon cooling, while single crystals of **2** and **3** were grown from slow evaporation of the NMR solutions.

Each of the structure solutions of **1-3** revealed a distorted square planar nickel center, bound to two halide atoms and chelated by the phosphorus atoms from a single **HL** ligand (Fig. 1). Selected bond lengths and angles are summarized in Table 2. The NH acts as a hydrogen bond donor to one halide in a neighboring molecule, giving rise to infinite 1-D chains in the solid state. The nitrogen atom of the ligand is bent slightly out of the NiP₂ plane by 0.146(2), 0.128(4), and 0.184(3) Å for **1-3**, respectively. In an ideal square planar coordination environment, the P

and X atoms would be co-planar, but in **1-3** the NiP₂ and NiX₂ planes were twisted relative to one another by 8.386(4), 7.521(7), and 15.158(4) °, respectively. The Ni-P bond lengths are unremarkable compared to previously reported nickel dihalides containing a P,P-chelating N-bridged ligand, whose mean value in the Cambridge Structural Database[11] is 2.123 Å (range 2.101-2.161 Å). The N-P bond lengths, however, fall at the short end of the range of 1.684-1.745 Å (mean 1.700 Å) for known structures.

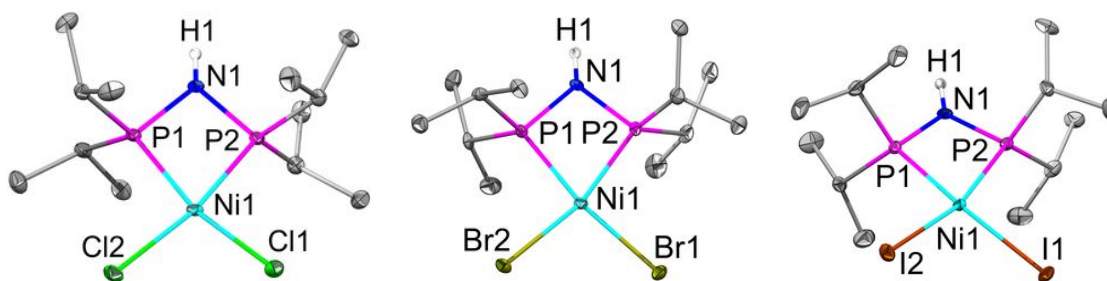


Fig. 1. Structures of (HL)NiX₂ complexes **1-3**. Thermal ellipsoids are shown at 50% probability and all hydrogen atoms except the N-H have been omitted for clarity.

Several different metal-ligand stoichiometries were screened during the preparations of **1-3**, but the 1:1 complexes appeared to be the only substances formed when the anion was a simple halide. By switching to more complex, weakly coordinating anions, it was possible to prepare a series of Ni²⁺ complexes with a different coordination environment. When warm ethanol solutions of the green-colored nickel salts Ni(BF₄)₂·6H₂O, Ni(NO₃)₂·6H₂O, or Ni(ClO₄)₂·6H₂O are combined in a 1:2 ratio with the neutral **HL** ligand HN[P(*i*-Pr)₂]₂ (Scheme 1), an immediate color change to orange-yellow occurs. Upon cooling, air- and moisture-stable yellow crystals with the formula [(HL)₂Ni]X₂ (X = BF₄ **4**; X = NO₃ **5**; X = ClO₄ **6**) are obtained in good yields. As was the case with **1**, these crystals obtained directly from the reaction mixture proved suitable for single crystal X-ray diffraction (Fig. 2).

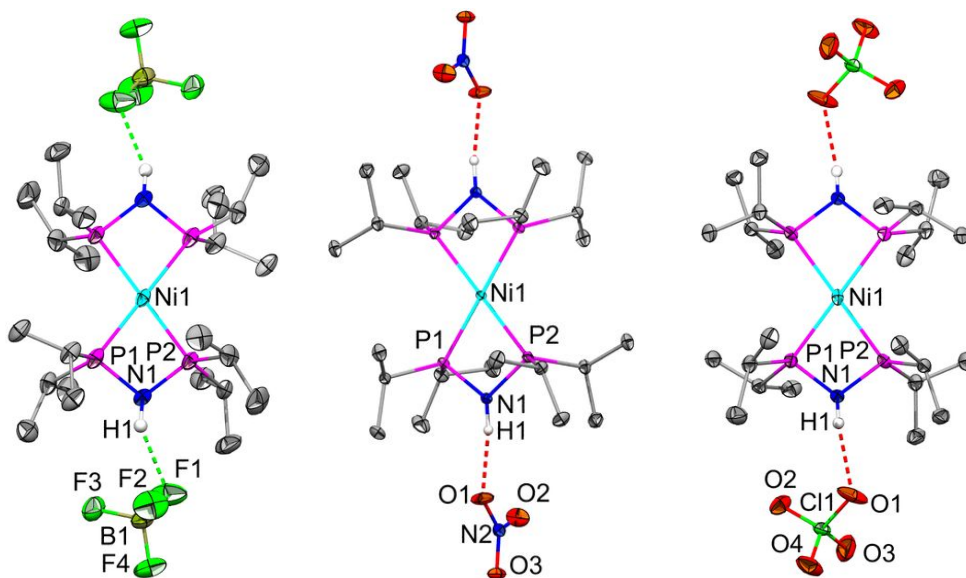


Fig. 2. Structures of $[(HL)_2Ni]X_2$ complexes **4-6**. Thermal ellipsoids are shown at 50% probability and all hydrogen atoms except the N-H have been omitted for clarity. Only the major position of the disordered BF_4 anion of **4** is shown.

As with complexes **1-3**, the structure solutions of **4-6** were very similar. Each one features a square planar Ni^{II} center chelated by the four phosphorus atoms of two **HL** ligands. Again, the nitrogen atom of the ligand is bent slightly out of the NiP_4 plane (**4** = 0.141(2) Å; **5** = 0.101(1) Å; **6** = 0.160(2) Å), similarly to the $(HL)NiX_2$ complexes **1-3**. In contrast to the hydrogen-bonded chains of **1-3**, each NH in **4-6** forms a hydrogen bond to a fluorine (**4**) or oxygen (**5, 6**) of the outer-sphere anions, and there are no notable supramolecular interactions beyond these discrete ion pairs. With the exception of the Ni-P bonds, which are on average nearly 0.1 Å longer in **4-6** than the corresponding bonds in **1-3**, there is little difference in between the bond lengths and angles across the six compounds (Table 2).

Despite the different metal-ligand ratios and anion coordination, the complexes **4-6** were surprisingly found to be just as poorly soluble as the original set, so once again only the $^1H\{^{31}P\}$ and $^{31}P\{^1H\}$ NMR spectra were recorded. Complexes **4** and **6** had nearly identical $^{31}P\{^1H\}$

spectra, each a singlet at 70.7 and 70.9 ppm, respectively, while **5** was found slightly upfield at 67.4 ppm. As was the case with the chloride and bromide compounds **1** and **2**, these resonances are very close to the signal of the free ligand, leaving the $^1\text{H}\{^{31}\text{P}\}$ NMR spectra as the best way to distinguish between product and starting material. Once again, the alkyl signals were shifted significantly downfield relative to the free ligand, with a single septet in each spectrum for the *CH* signal between 2.43-2.44 ppm for each of **4-6**, while the two *CH*₃ doublets were recorded between 1.35-1.37 and 1.46-1.47 ppm. For **HL**, the corresponding resonances are 1.61, 1.06, and 1.03 ppm, respectively. Despite the similarities in the alkyl region of their NMR spectra, the *NH* signal varied substantially from one complex to the next. For compounds **4** and **6**, the *NH* resonance appears at 5.75 ppm and 6.01 ppm, respectively, significantly downfield from the corresponding signals in **1-3** (3.07-3.27 ppm). Compound **5** is even more of an outlier, found at 8.36 ppm. A similar pattern was seen in the IR spectra. The *NH* stretches of **4** and **6** were found at 3244 and 3150 cm^{-1} , respectively, close to those of **1-3** (3186-3202 cm^{-1}), but **5** was quite different at 2569 cm^{-1} . This is a region more typically associated with cationic *NH* groups.[26] Of the six complexes, **5** has the shortest *N-H*•••*X* hydrogen bond, which is perhaps why its *NH* stretch has such a different spectroscopic signature.

As we noted earlier, complexes containing neutral **HL** were heretofore virtually unknown, but the use of it and related $\text{HN}(\text{PR}_2)_2$ ligands in their anionic form $[\text{N}(\text{PR}_2)_2]^-$ is relatively widespread. **HL** can be deprotonated *in situ* by NaNH_2 in Et_2O . Subsequent addition of NiI_2 gives, after 24 hours, L_2Ni **7** (Scheme 2). The orange crystals of **7** were far more soluble than complexes **1-6**, allowing for characterization by $^{13}\text{C}\{^1\text{H}\}$ NMR spectroscopy as well as $^1\text{H}\{^{31}\text{P}\}$ and $^{31}\text{P}\{^1\text{H}\}$ NMR spectroscopy. A single isopropyl environment was observed, with

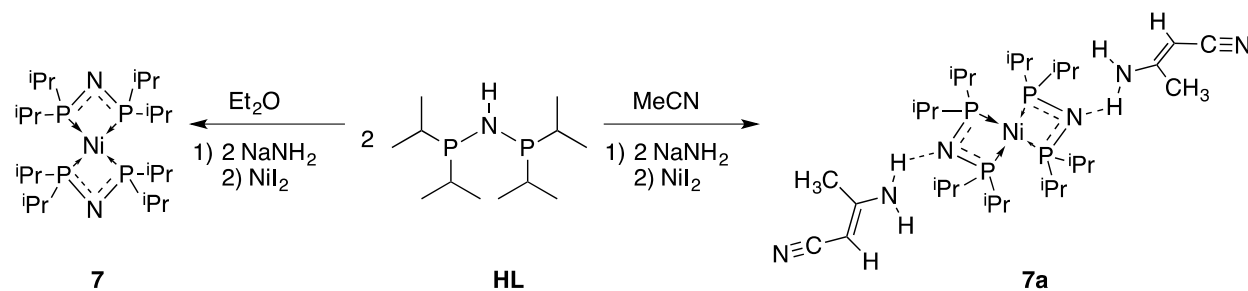
the CH and CH₃ fragments at 1.88, 1.41, and 1.15 ppm in the ¹H{³¹P} NMR spectrum, and at 30.9,

Table 2. Selected bond lengths (Å) and angles (°) of the nickel complexes **1-8**.

1	2	3	4	5	6	7	7a	8
	2.1340(5)	2.1330(11)	2.1463(8)	2.2558(8)	2.2047(3)	2.2344(6)	2.2280(2)	2.2266(6) 2.1713(4) 2.2199(5) 2.1723(4)
	2.1325(5)	2.1354(11)	2.1443(8)	2.2089(6)	2.2274(3)	2.2499(6)	2.2380(3)	2.2172(5) 2.1891(4) 2.2273(6) 2.1885(4)
	1.6871(15)	1.684(3)	1.688(3)	1.684(2)	1.6877(9)	1.682(2)	1.6561(9)	1.6632(16) 1.7076(14) 1.6680(17) 1.7096(13)
	1.6834(15)	1.683(3)	1.681(3)	1.688(2)	1.6837(9)	1.676(2)	1.6582(9)	1.6626(17) 1.7167(13) 1.6628(17) 1.7162(13)
	3.4091(16)	3.616(3)	3.646(2)	2.890(3)	2.7886(13)	2.884(3)		
	97.97(8)	98.73(17)	98.75(13)	102.31(12)	101.87(5)	102.97(11)	96.95(5)	96.46(9) 101.82(7) 96.78(9) 101.66(7)
	73.177(18)	73.55(4)	73.16(3)	72.07(2)	72.398(10)	71.75(2)	67.502(9)	67.860(19) 75.108(16) 68.106(19) 75.043(16)
			107.93(2)	107.601(10)	108.25(2)	112.498(9)	111.73(2) 112.12(2)	
	156.(2)	162.(4)	170.(3)	153.(3)	167.6(14)	169.(3)		

	Ni1-P1	Ni1-P2	P1-N1	P2-N1	N...X	P1-N1-P2	P1-Ni1-P2	P1-Ni1-P2'	N-H...X
--	--------	--------	-------	-------	-------	----------	-----------	------------	---------

19.0, and 16.7 ppm in the $^{13}\text{C}\{^1\text{H}\}$ NMR spectrum. Likewise, a single $^{31}\text{P}\{^1\text{H}\}$ peak was observed, with the somewhat unexpected chemical shift of 24.3 ppm. This is far upfield from the previously reported complexes featuring anionic L^- as either a P,P-chelating ligand in L_2Zn (91.4 ppm),^[16] L_2Sn (80.2 ppm),^[17] L_2SnCl_2 (127.1 ppm)^[27] and L_2InCl (122 ppm)^[18] or as a P,P-bridging ligand in $(\text{LSn})_2$ or $(\text{LGe})_2$ at 98.3 and 103.5 ppm, respectively.^[27]



Scheme 2. Synthesis of L_2Ni **7** and $\text{L}_2\text{Ni}\cdot 2[\text{NCCHC}(\text{Me})\text{NH}_2]$ **7a**.

The structure of **7** was confirmed by single crystal X-ray diffraction (Fig. 3). The square planar Ni^{II} ion is P,P-chelated by two ligands, just as in the cores of the $[(\text{HL})_2\text{Ni}]\text{X}_2$ complexes **4-6**. Although one might expect the Ni-P bonds to be shorter with an anionic rather than a neutral ligand, they are instead quite similar in length to **4-6**. The P-N bonds, however, are slightly shorter and the P-N-P and P-Ni-P (chelate) angles are more acute than any found in **1-6**.

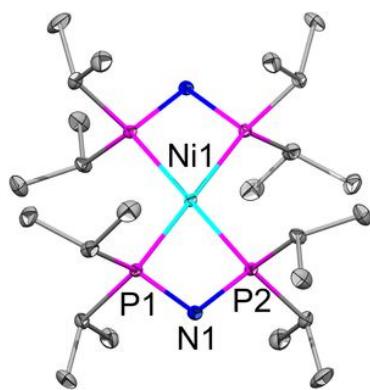


Fig. 3. Structure of L_2Ni complex **7**. Thermal ellipsoids are shown at 50% probability and hydrogen atoms have been omitted for clarity.

Because **7** took significantly longer to form than the neutral-ligand complexes **1-6**, a number of different solvents and deprotonating agents were screened in an attempt to improve the reaction rate. Initially, acetonitrile appeared to be a much better solvent than the diethyl ether for this synthesis. By $^{31}P\{^1H\}$ NMR spectroscopy, the conversion was complete in about four hours instead of twenty four hours, and the yield of orange powder after work-up was higher. Further characterization, however, indicated that it was not pure **7** that had been isolated from the MeCN solution. The melting point of this product **7a** was significantly lower and both the $^1H\{^{31}P\}$ and $^{13}C\{^1H\}$ NMR spectra had, in addition to the peaks that corresponded to **7**, extra peaks that were inconsistent with either **HL** or the reaction solvent. To determine the nature of this product, single crystals of **7a** were grown from a concentrated CH_2Cl_2 solution.

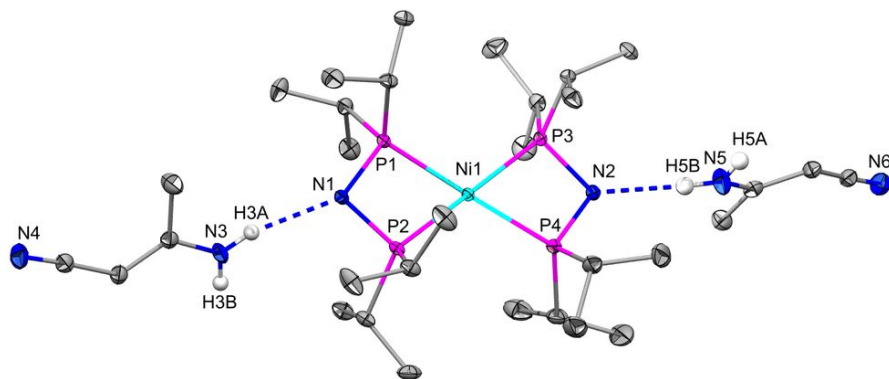


Fig. 4. Structure of $L_2Ni \cdot 2[NCCHC(Me)NH_2]$ **7a**. Thermal ellipsoids are shown at 50% probability and all hydrogen atoms except the N-H have been omitted for clarity.

The structure was solved as a 1:2 co-crystal of **7** and 3-amino-2-butenitrile, also known as 3-aminocrotonitrile (Fig. 4). In addition to deprotonating **HL**, the $NaNH_2$ quite unexpectedly promotes a Thorpe reaction[28] of the acetonitrile solvent, thus leading to the formation of the 3-amino-2-butenitrile. This molecule engages in extensive hydrogen-bonding (Fig. 5), preventing its removal during normal work-up procedures. The amine end of the 3-amino-2-butenitrile acts as a hydrogen bond donor, and the nitrile end acts as an acceptor, forming infinite chains with itself. These chains are cross-linked by the nickel complex whose deprotonated N atoms also behave as hydrogen bond acceptors; interestingly, the opposite role that they play in their neutral form in **1-6**. Despite its versatility in hydrogen bonding, being known since at least 1889,[29] and being commercially available from several suppliers, crystal structures containing 3-amino-2-butenitrile have been reported only twice before – once as a co-crystal with tetramethylammonium fluoride[30] and just last year as the discrete molecule.[31]

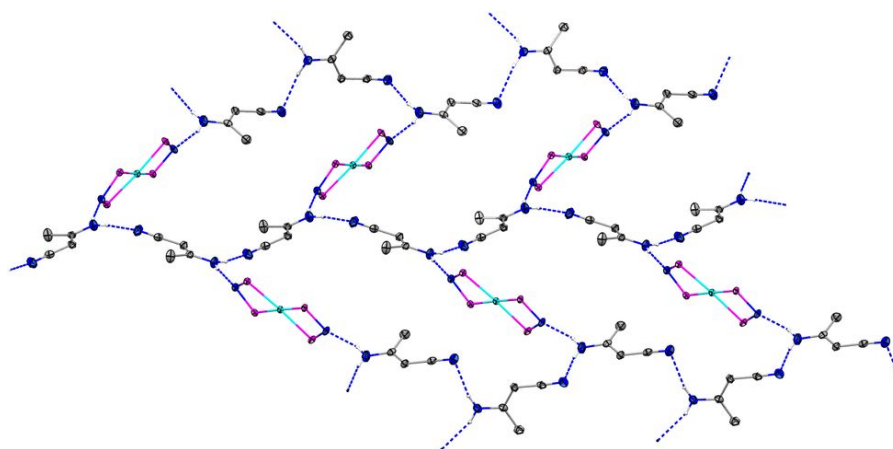
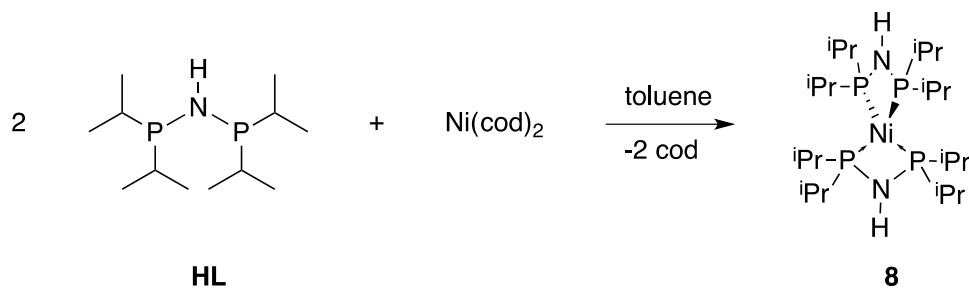


Fig. 5. Hydrogen-bonding in **7a**. Isopropyl groups omitted for clarity.

Although Ni^{II} is the oxidation state for many of the applications noted in the introduction, Ni⁰ is also very commonly used. Using a ligand closely related to **HL**, namely HN(PPh₂)₂, Kornev *et al.* reported that they were unable to obtain the corresponding homoleptic Ni⁰ complex from Ni(cod)₂ but they were able to isolate a heteroleptic complex [HN(PPh₂)₂]₂Ni(PPh₃)₂. [13a] Kubiak *et al.* found that in the presence of various isocyanides, the reaction of Ni(cod)₂ and HN(PPh₂)₂ also gives heteroleptic complexes, although in that case the HN(PPh₂)₂ ligands bridged two metal centers instead of acting as a chelate to a single nickel atom. [32]

In light of those precedents, we were unsure what to expect from the reaction of Ni(cod)₂ with two equivalents of **HL** (Scheme 3). The reaction was monitored by ³¹P{¹H} NMR spectroscopy which showed the clean formation of a single product **8** over the course of a few hours. This is consistent with our prior observations (*vide supra*) that there is often a great difference in reactivity when phenyl substituents are replaced with isopropyl groups. The ³¹P{¹H} NMR spectrum of **8** is a singlet at 97.9 ppm, the most downfield of all the compounds described herein. In the ¹H{³¹P} spectrum, the signals assigned to the isopropyl CH and CH₃ groups were observed as a septet at 1.90 and doublets at 1.21 and 1.23 ppm. Consistent with an absence of hydrogen bond acceptors, the NH was found at 1.72 ppm in the NMR spectrum and 3323 cm⁻¹ in the IR spectrum. Neither the ¹H{³¹P} nor the ¹³C{¹H} spectra showed any resonances corresponding to cyclooctadiene, suggesting that **8** was a homoleptic species.



Scheme 3. Synthesis of the Ni⁰ complex **8**.

Since **HL** and Ni(cod)₂ were combined in a 2:1 ratio and no unreacted ligand was found to persist in the crude reaction mixture, it seemed most likely that **8** was a chelate complex of the form (HL)₂Ni, rather than a P,P-bridged [(HL)Ni]₂. Single crystals were grown from a concentrated pentane solution and the structure was confirmed as (HL)₂Ni (Fig. 6). As one would expect upon switching from the d⁸ Ni^{II} centers of **1-7a** to the d¹⁰ Ni⁰ configuration of **8**, the coordination geometry at nickel is now tetrahedral instead of square planar. The Ni-P bond lengths (Table 2) are within the range of those noted for **1-7a**, despite the difference in charge at the metal center. The P-N bonds, however, are not only longer than in the other complexes, but are slightly longer on average than in the free ligand[17] itself (**HL** = 1.705(4) Å, **8** = average 1.712(13) Å). This is consistent with backbonding between the Ni⁰ and P weakening the P-N bonds.

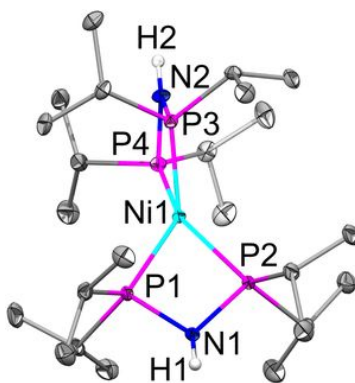


Fig. 6. Structure of (HL)₂Ni complex **8**. Thermal ellipsoids are shown at 50% probability and all hydrogen atoms except the N-H have been omitted for clarity.

3.2 Electrochemistry

Compounds **1**, **2**, and **3** display very similar cathodic behaviors. For each compound at least four modestly spaced diffusion-controlled *chemically*-irreversible cathodic reductions were observed at the potentials collected in Table 3. Some smaller oxidation waves were also observed during the back scan and those are presumably due to the presence of decomposed reduced products (Fig. 7-9). No peak was observed in the oxidative region.

Bulk coulometry at the potential of the first cathodic wave confirmed that the first redox event is a one-electron process. Unfortunately, the rapid decomposition of the mono-electronically reduced product did not allow identification of its structure. The peak potential of the first reduction wave decreases when chloride (**1**) is replaced by bromide (**2**), and is even lower when replaced by iodide (**3**). This tends to suggest that the electrochemical reduction of those compounds involve the reduction of the metal-halogen bond as the first step.[33] Although the formation of a transient **1**⁻, **2**⁻, or **3**⁻ could not be ruled out, the lack of reversibility of the first reduction at higher sweeping rates (up to 250,000 V.s⁻¹) and at low temperature (-50°C) suggests that the electron transfer might be coupled to the cleavage of the nickel-halogen bond. In addition to the *chemical* irreversibility, **1**, **2** as well as **3** display an important degree of *electrochemical* irreversibility.[34] The measured E_p-E_{p/2} values for the first reduction of these complexes are diagnostic of a slow charge transfer process with coefficient (α) of 0.28, 0.34, and 0.37, respectively.[34] Finally, in presence of CO₂, no change has been observed during the cyclic voltammetry and bulk electrolysis experiments.

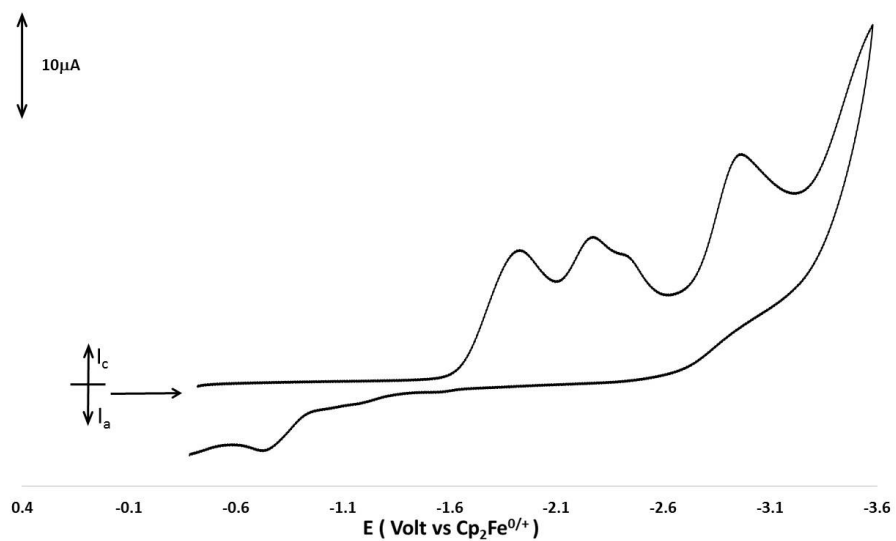


Figure 7. Cyclic Voltammetry scan of 1 mM **1** in THF/0.1M [NBu₄][PF₆] at 3 mm glassy carbon electrode, scan rate 0.2V s⁻¹.

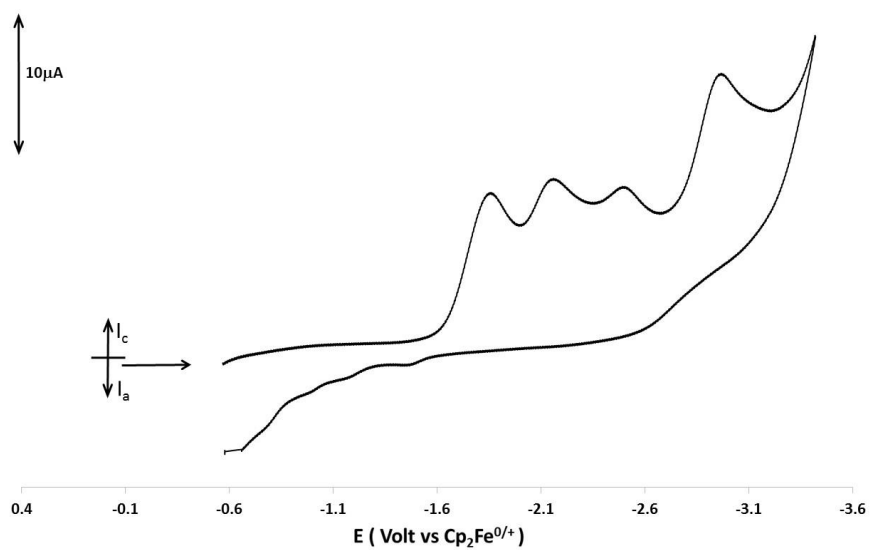


Figure 8. Cyclic Voltammetry scan of 1 mM **2** in THF/0.1M [NBu₄][PF₆] at 3 mm glassy carbon electrode, scan rate 0.2V s⁻¹.

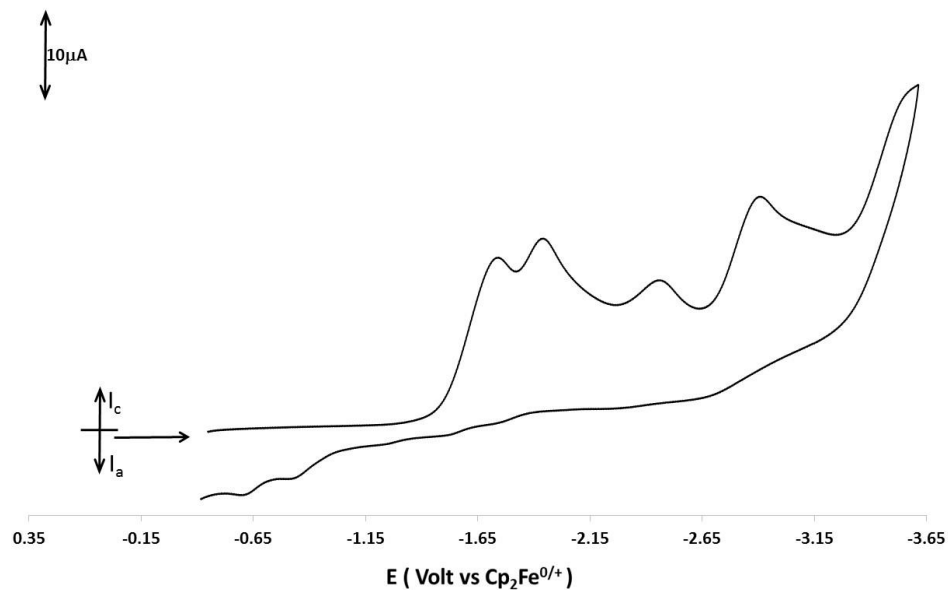


Figure 9. Cyclic Voltammetry scan of 1 mM **3** in THF/0.1M [NBu₄][PF₆] at 3 mm glassy carbon electrode, scan rate 0.2V s⁻¹.

Table 3. Electrochemical parameters for compounds **1**, **2** and **3**.

Compound	First reduction	E _p -E _{p/2}	Second reduction	Third reduction	Fourth reduction
1	E _{pc} = -1.93 V	170 mV	E _{pc} = -2.28 V	E _{pc} = -2.44 V	E _{pc} = -2.97 V
2	E _{pc} = -1.86 V	140 mV	E _{pc} = -2.16 V	E _{pc} = -2.50 V	E _{pc} = -2.96 V
3	E _{pc} = -1.73V	130 mV	E _{pc} = -1.94 V	E _{pc} = -2.46 V	E _{pc} = -2.91 V

Compounds **4**, **5**, and **6** display again very similar redox behaviors. Although only compound **6** proved to be totally soluble under our electrochemical conditions, **4** and **5** were soluble enough to yield reliable electrochemical data. Each of the complexes demonstrates two reduction waves with significant chemical reversibility, which is consistent with the reduction of the nickel center from Ni^{II} to Ni^I and then from Ni^I to Ni⁰. The E_{1/2} values for those oxidations

are very similar for each complex and are summarized in Table 4. More over, bulk electrolysis of compound **6**, under argon atmosphere, at -1.30 V and at -1.60 V confirmed that both reduction processes involve a one-electron transfer. In addition, the Ni^I and Ni⁰ reduced forms of the complex have been found to be stable under the bulk electrolysis conditions since their re-oxidation led to the quantitative reformation of the starting material.

Table 4. Electrochemical parameters for compounds **4**, **5** and **6**.

Compound	E ¹ _{pc}	E ¹ _{pa}	E ¹ _{1/2}	E ² _{pc}	E ² _{pa}	E ² _{1/2}
4	-1.04 V	-0.90 V	-0.97 V	-1.51 V	-1.39 V	-1.45 V
5	-1.13 V	-0.99	-1.06 V	-1.59 V	-1.47 V	-1.53 V
6	-1.11V	-0.91 V	-1.01 V	-1.56 V	-1.42 V	-1.49 V

In presence of CO₂, cyclic voltammograms of compounds **4**, **5**, and **6** exhibit significantly different features showing a reaction between the low valent compound and carbon dioxide (Table 5). The fact that the reduction potentials for the two redox events are similar to those previously recorded in absence of CO₂ suggests that the compounds are unlikely to spontaneously form a CO₂ adduct prior to their reduction. More specifically, for complexes **5** and **6**, no change was observed to the first reduction process when scanning until -1.20 V. However, scanning past the second reduction wave showed a complete loss of chemical reversibility for both reductions as well as a significant increase of current for the second reduction wave. This indicates that the Ni⁰ form of the complex is reacting with CO₂ and proceeds presumably via an outer-sphere process.[35] Surprisingly, in the case of compound **4**, both reduction waves showed an increase of current under CO₂ conditions suggesting a more intricate mechanism. As expected, chemical reversibility as well as the original electrochemical features of each compounds were restored after purging the solution with argon. Bulk electrolysis of compound **6**

at -1.6V under CO₂ never reached completion even after passing 9F/mol. However, when the bulk electrolysis cell was purged with argon and the electrolysis resumed, the cathodic reduction of compound **6** was achieved after passing 2F/mol. This suggest that the reduced form of the catalyst is able to perform catalytical electroreduction of CO₂.

Efforts are underway to fully characterize the products of the irreversible oxidations in presence of CO₂.

Table 5. Electrochemical parameters for compounds **4**, **5** and **6** in presence of CO₂

Compound	E_{pc}^1	I_{pccat}^1/I_{pc0}	E_{pc}^2	I_{pccat}^2/I_{pc0}
4	-1.14 V	6.6	-1.79V	6.6
5	-1.13 V	/	-1.59 V	14.4
6	-1.11V	/	-1.56 V	2.0

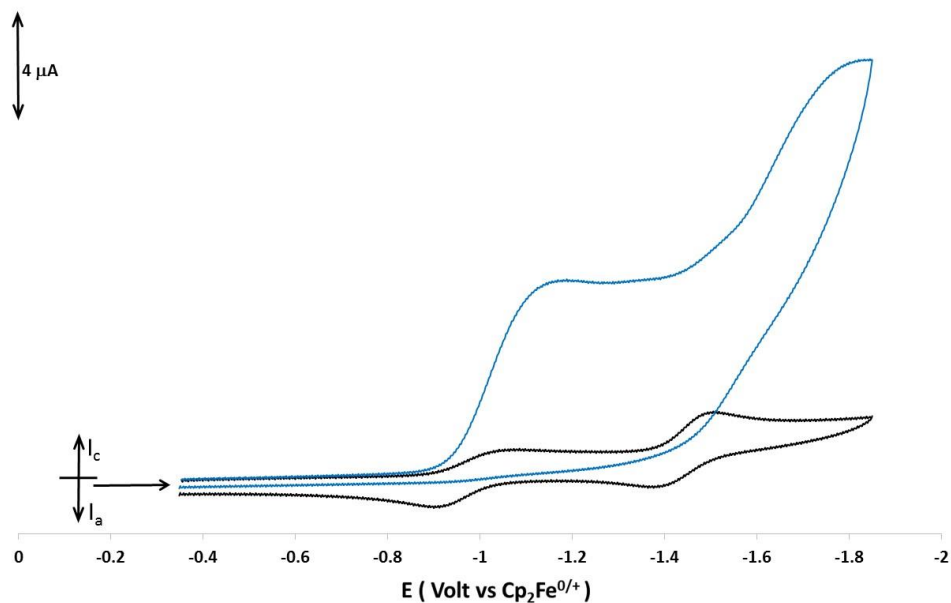


Figure 10. Cyclic Voltammetry scan of **4** in THF/0.1M [NBu₄][PF₆] at 3 mm glassy carbon electrode, scan rate 0.2V s⁻¹ under argon (black curve) and under CO₂ (blue curve) atmosphere.

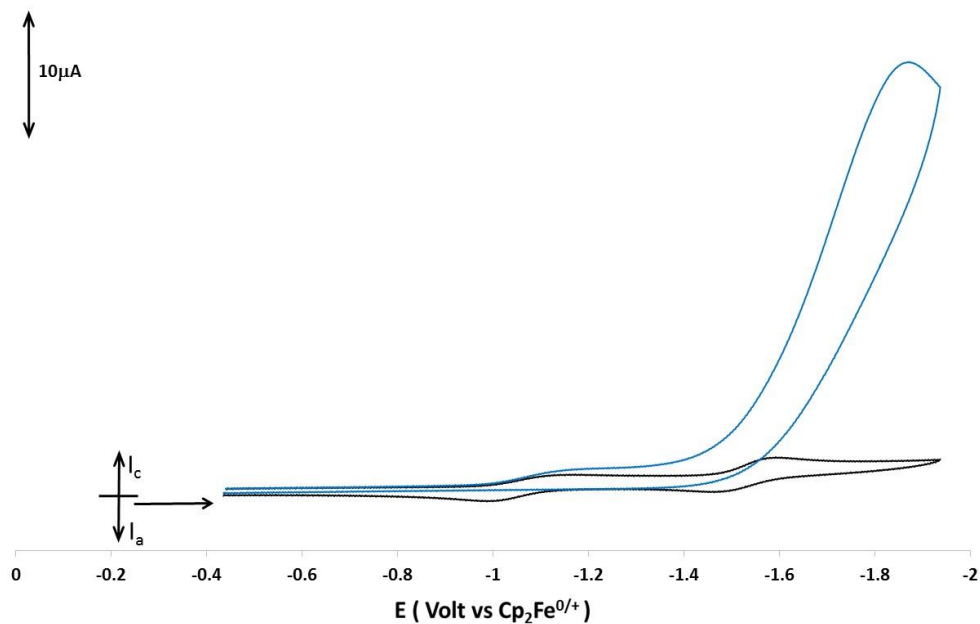


Figure 11. Cyclic Voltammetry scan of **5** in THF/0.1M [NBu₄][PF₆] at 3 mm glassy carbon electrode, scan rate 0.2V s⁻¹ under argon (black curve) and under CO₂ (blue curve) atmosphere.

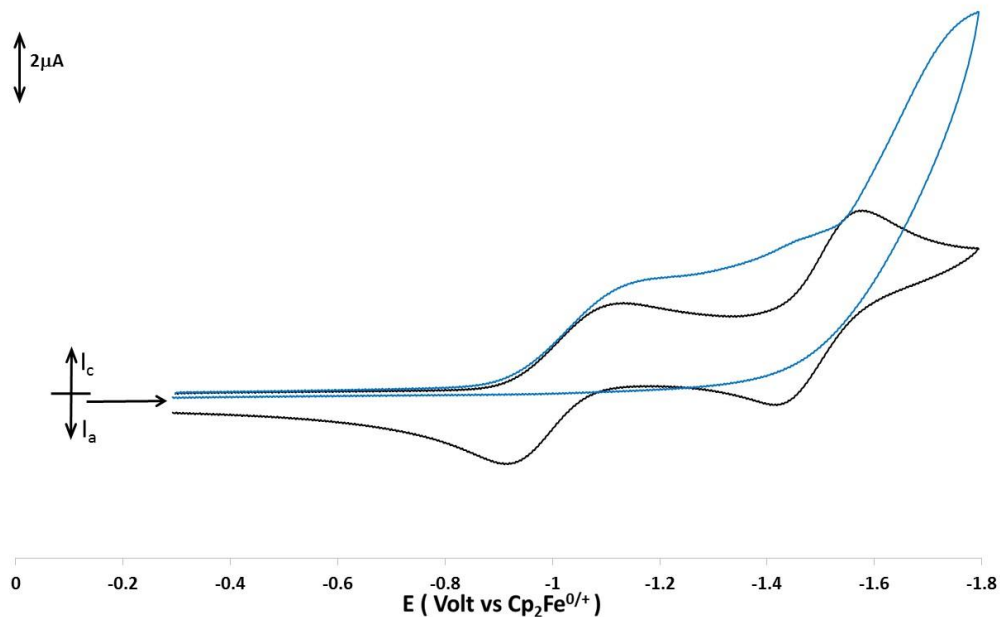


Figure 12. Cyclic Voltammetry scan of 1mM **6** in THF/0.1M [NBu₄][PF₆] at 3 mm glassy carbon electrode, scan rate 0.2V s⁻¹ under argon (black curve) and under CO₂ (blue curve) atmosphere.

4. CONCLUSIONS

Six air- and moisture-stable Ni^{II} complexes of bis(diisopropylphosphino)amine (**HL**) were prepared from either a 1:1 ratio of **HL** with NiCl₂•6H₂O, NiBr₂, and NiI₂, or a 2:1 ratio of **HL** with Ni(BF₄)₂•6H₂O, Ni(NO₃)₂•6H₂O, and Ni(ClO₄)₂•6H₂O, all in ethanol solutions. The resulting complexes, which took the form of either (**HL**)NiX₂ (X = Cl, Br, I) or [(**HL**)₂Ni]X₂ (X = BF₄, NO₃, ClO₄), were characterized by IR and multi-nuclear NMR spectroscopy as well as single-crystal X-ray diffraction. In tests of their ability to act as electrocatalysts for the reduction of CO₂, the simple halides (**HL**)NiX₂ (X = Cl, Br, I) were found to undergo chemical and electrochemical irreversible reductions. Electrocatalytic reduction of CO₂ was possible with the [(**HL**)₂Ni]X₂ (X = BF₄, NO₃, ClO₄) complexes. The synthesis and characterization of the Ni⁰

complex $(\mathbf{HL})_2\text{Ni}$ and the Ni^{II} complexes $\mathbf{L}_2\text{Ni}$ and $\mathbf{L}_2\text{Ni}\cdot 2[\text{NCCHC}(\text{Me})\text{NH}_2]$ were also described.

Acknowledgments

Dr. Beth Donovan (UNM) and Mr. Nate Wilson (SNL) performed preliminary electrochemical experiments on **5**. Mr. Jeremiah Sears (SNL) performed the elemental analysis on compounds **7** and **7a**. This work was financially supported by the National Science Foundation (Grant CHE12-13529), the Sandia National Laboratories-sponsored STAR Summer Fellows program, and the Kazakh Ministry of Education and Science. The Bruker X-ray diffractometer was purchased via a National Science Foundation CRIF:MU award to the University of New Mexico (CHE04-43580), and the NMR spectrometers were upgraded via grants from the NSF (CHE08-40523 and CHE09-46690). Sandia is a multiprogram laboratory operated by Sandia Corporation, a Lockheed Martin Company, for the U.S. Department of Energy's National Nuclear Security Administration under Contract DE-AC04-94-AL85000.

Appendix A. Supplementary Material

CCDC 1477634-1477642 contain the supplementary crystallographic data for complexes **1-8**. These data can be obtained free of charge via <http://www.ccdc.cam.ac.uk/conts/retrieving/html>, or from the Cambridge Crystallographic Data Centre, 12 Union Road, Cambridge CB2 1EZ, UK; fax: +44 1223 336 033; or e-mail: deposit@ccdc.cam.ac.uk.

References

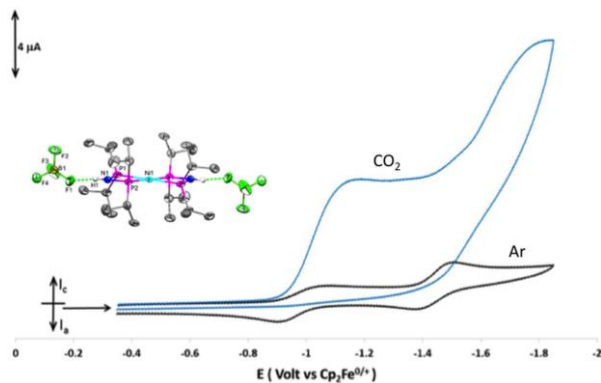
- [1] E.A. LaPierre, W.E. Piers, D.M. Spasyuk, D.W. Bi, *Chem. Commun.*, 52 (2016) 1361-1364.
- [2] A.N. Desnoyer, E.G. Bowes, B.O. Patrick, J.A. Love, *J. Am. Chem. Soc.*, 137 (2015) 12748-12751.

- [3] K.T. Horak, S. Lin, J. Rittle, T. Agapie, *Organometallics*, 34 (2015) 4429-4432.
- [4] T. Rosser, M.A. Gross, Y.-H. Lai, E. Reisner, *Chem. Sci.*, (2016) 10.1039/c1035sc04863j.
- [5] (a) M. Schultz, F. Eisenträger, C. Regius, F. Rominger, P. Hanno-Igels, P. Jakob, I. Gruber, P. Hofmann, *Organometallics*, 31 (2012) 207-224; (b) P. Boulens, M. Lutz, E. Jeanneau, H. Olivier-Bourbigou, J.N.H. Reek, P.-A.R. Breuil, *Eur. J. Inorg. Chem.*, (2014) 3754-3762; (c) A. Ghisolfi, C. Fliedel, V. Rosa, K.Y. Monakhov, P. Braunstein, *Organometallics*, 33 (2014) 2523-2534.
- [6] (a) A. Mifleur, H. Ledru, A. Lopes, I. Suisse, A. Mortreux, M. Sauthier, *Adv. Synth. Catal.*, 358 (2016) 110-121; (b) Y. Kita, R. Kavthe, H. Oda, K. Mashima, *Angew. Chem. Int. Ed.*, 55 (2016) 1098-1101; (c) E.A. Standley, S.J. Smith, P. Müller, T.F. Jamison, *Organometallics*, 33 (2014) 2012-2018; (d) M. Shevlin, M.R. Friedfeld, H. Sheng, N.A. Pierson, J.M. Hoyt, L.-C. Campeau, P.J. Chirik, *J. Am. Chem. Soc.*, 138 (2016) 3562-3569.
- [7] X. Wu, Y. Zhao, H. Ge, *J. Am. Chem. Soc.*, 136 (2014) 1789-1792.
- [8] (a) X. Hong, Y. Liang, K.N. Houk, *J. Am. Chem. Soc.*, 136 (2014) 2017-2025; (b) A. Arévalo, A. Tlahuext-Aca, M. Flores-Alamo, J.J. García, *J. Am. Chem. Soc.*, 136 (2014) 4634-4639; (c) L. Gan, T.L. Groy, P. Tarakeshwar, S.K.S. Mazinani, J. Shearer, V. Mujica, A.K. Jones, *J. Am. Chem. Soc.*, 137 (2015) 1109-1115; (d) R.C. Cammarota, C.C. Lu, *J. Am. Chem. Soc.*, 137 (2015) 12486-12489; (e) A. Kruckenberg, H. Wadepohl, L.H. Gade, *Organometallics*, 32 (2013) 5153-5170; (f) B.R. Galan, E.S. Wiedner, M.L. Helm, J.C. Linehan, A.M. Appel, *Organometallics*, 33 (2014) 2287-2294; (g) A. Ghisolfi, F. Condello, C. Fliedel, V. Rosa, P. Braunstein, *Organometallics*, 34 (2015) 2255-2260.
- [9] (a) P.N. Plessow, L. Weigel, R. Lindner, A. Schäfer, F. Rominger, M. Limbach, P. Hofmann, *Organometallics*, 32 (2013) 3327-3338; (b) R. Fischer, J. Langer, A. Malassa, D. Walther, H. Görls, G. Vaughn, *Chem. Commun.*, (2006) 2510-2512; (c) L. Xue, M.S.G. Ahlquist, *Inorg. Chem.*, 53 (2014) 3281-3289; (d) R. Beck, M. Shoshani, J. Krasinkiewicz, J.A. Hatnean, S.A. Johnson, *Dalton Trans.*, 42 (2013) 1461-1475; (e) P.N. Plessow, A. Schäfer, M. Limbach, P. Hofmann, *Organometallics*, 33 (2014) 3657-3668; (f) L. González-Sebastián, M. Flores-Alamo, J.J. García, *Organometallics*, 34 (2015) 763-769.
- [10] (a) A.M. Appel, J.E. Bercaw, A.B. Bocarsly, H. Dobbek, D.L. Dubois, M. Dupuis, J.G. Ferry, E. Fujita, R. Hille, P.J.A. Kenis, C.A. Kerfeld, R.H. Morris, C.H.F. Peden, A.R. Portis, S.W. Ragsdale, T.B. Rauchfuss, J.N.H. Reek, L.C. Seefeldt, R.K. Thauer, G.L. Waldrop, *Chem. Rev.*, 113 (2013) 6621-6658; (b) Z. Yuan, M.R. Eden, R. Gani, *Ind. Eng. Chem. Res.*, 55 (2016) 3383-3419; (c) P. Kang, Z. Chen, M. Brookhart, T.J. Meyer, *Top. Catal.*, 58 (2015) 30-45; (d) G. Neri, I.M. Aldous, J.J. Walsh, L.J. Hardwick, A.J. Cowan, *Chem. Sci.*, 7 (2016) 1521-1526; (e) Q. Liu, L. Wu, R. Jackstell, M. Beller, *Nature communications*, 6 (2015) 5933; (f) G.A. Olah, G.K. Prakash, A. Goepfert, *J. Am. Chem. Soc.*, 133 (2011) 12881-12898; (g) R. Kortlever, J. Shen, K.J.P. Schouten, F. Calle-Vallejo, M.T.M. Koper, *J. Phys. Chem. Lett.*, 6 (2015) 4073-4082; (h) S. Sato, T. Arai, T. Morikawa, *Inorg. Chem.*, 54 (2015) 5105-5113; (i) G. Sahara, O. Ishitani, *Inorg. Chem.*, 54 (2015) 5096-5104; (j) D.L. Dubois, *Inorg. Chem.*, 53 (2014) 3935-3960; (k) M. Mikkelsen, M. Jørgensen, F. Krebs, *Energy Environ. Sci.*, 3 (2010) 43-81; (l) D. Pletcher, *Electrochem. Commun.*, 61 (2015) 97-101; (m) J. Qiao, Y. Liu, F. Hong, J. Zhang, *Chem. Soc. Rev.*, 43 (2014) 631-675; (n) C. Costentin, M. Robert, J.-M. Savéant,

- Chem. Soc. Rev., 42 (2013) 2423-2436; (o) M. Aresta, A. Dibenedetto, A. Angelini, Chem. Rev., 114 (2014) 1709-1742; (p) L.J. Murphy, K.N. Robertson, R.A. Kemp, H.M. Tuononen, J.A.C. Clyburne, Chem. Commun., 51 (2015) 3942-3956; (q) U.-P. Apfel, W. Weigand, Angew. Chem. Int. Ed., 50 (2011) 4262-4264.
- [11] C.R. Groom, F.H. Allen, Angew. Chem. Int. Ed., 53 (2014) 662-671.
- [12] A. Grabulosa, S. Doran, G. Brandariz, G. Muller, J. Benet-Buchholz, A. Riera, X. Verdaguer, Organometallics, 33 (2014) 692-701.
- [13] (a) V.V. Sushev, A.N. Kornev, Y.V. Fedotova, Y.A. Kursky, T.G. Mushtina, G.A. Abakumov, L.N. Zakharov, A.L. Rheingold, J. Organomet. Chem., 676 (2003) 89-93; (b) V.V. Sushev, A.N. Kornev, Y.A. Kurskii, O.V. Kuznetsova, G.K. Fukin, Y.H. Budnikova, G.A. Abakumov, J. Organomet. Chem., 69 (2005) 1814-1821.
- [14] D.A. Dickie, R.A. Kemp, Acta Crystallogr. Sect. E: Struct. Rep. Online, E64 (2008) o1449.
- [15] D.A. Dickie, M.V. Parkes, R.A. Kemp, Angew. Chem. Int. Ed., 47 (2008) 9955-9957.
- [16] D.A. Dickie, R.A. Kemp, Organometallics, 33 (2014) 6511-6518.
- [17] D.A. Dickie, E.N. Coker, R.A. Kemp, Inorg. Chem., 50 (2011) 11288-11290.
- [18] D.A. Dickie, M.T. Barker, M.A. Land, K.E. Hughes, J.A.C. Clyburne, R.A. Kemp, Inorg. Chem., 54 (2015) 11121-11126.
- [19] J.S. Ritch, T. Chivers, K. Ahmad, M. Afzaal, P. O'Brien, Inorg. Chem., 49 (2010) 1198-1205.
- [20] Bruker AXS, Inc., Madison, Wisconsin, USA (2015).
- [21] G. Gritzner, J. Kůta, Pure Appl. Chem., 56 (1984) 461-466.
- [22] R.R. Gagné, C.A. Koval, G.C. Lisensky, Inorg. Chem., 19 (1980) 2854-2855.
- [23] B.M. Barry, D.A. Dickie, L.J. Murphy, J. Clyburne, R.A. Kemp, Inorg. Chem., 52 (2013) 8312-8314.
- [24] P. Stoessel, D. Joosten, E. Breuning, H. Yersin, U. Monkowius, in, Merck Patent GmbH, Germany . 2010, pp. 80pp.
- [25] A.M.Z. Slawin, M.B. Smith, J.D. Woollins, J. Chem. Soc., Dalton Trans., (1997) 1877-1881.
- [26] C.J. Pouchert, The Aldrich Library of Infrared Spectra. 3rd Ed, Aldrich Chem. Co., 1981.
- [27] C.J. Miller, U. Chadha, J.R. Ulibarri-Sanchez, D.A. Dickie, R.A. Kemp, Polyhedron, 114 (2016) 351-359.
- [28] J. March, Advanced Organic Chemistry: Reactions, Mechanisms and Structure, 4th ed., Wiley & Sons, New York, 1992.
- [29] R. Holtzwardt, J. Prakt. Chem., 39 (1889) 230-245.
- [30] K.O. Christe, W.W. Wilson, R.D. Wilson, R. Bau, J.-a. Feng, J. Am. Chem. Soc., 112 (1990) 7619-7625.
- [31] A.L. Rheingold, M. Gembicky, CCDC 1428277: Private communication to the Cambridge Structural Database (2015), DOI: 10.5517/cc1jy7g5.
- [32] E. Simón-Manso, C.P. Kubiak, Organometallics, 24 (2005) 96-102.
- [33] R.J. Enemaerke, J. Larsen, T. Skrydstrup, K. Daasbjerg, Organometallics, 23 (2004) 1866-1874.
- [34] In practical terms, electrochemical reversibility (also termed Nernstian behavior) refers to the speed of charge-transfer in a redox reaction, whereas chemical reversibility refers to follow-up reactions that accompany the charge-transfer process. For an introductory discussion of these terms, see Bard, A. J.; Faulkner, L. N., *Electrochemical Methods*, John Wiley & Sons, New York, **2001**, 2nd Ed., pp 35-38 and pp 44-49).

[35] R.J. Haines, R.E. Wittrig, C.P. Kubiak, *Inorg. Chem.*, 33 (1994) 4723-4728.

Graphical Abstract:



Bis(diisopropylphosphino)amine (HL) reacts with NiX_2 ($\text{X} = \text{Br}, \text{I}$) and $\text{NiX}_2 \cdot 6\text{H}_2\text{O}$ ($\text{X} = \text{Cl}, \text{BF}_4, \text{NO}_3, \text{ClO}_4$) to form P,P-chelated complexes $(\text{HL})\text{NiX}_2$ ($\text{X} = \text{Cl}, \text{Br}, \text{I}$) and $[(\text{HL})_2\text{Ni}]\text{X}_2$ ($\text{X} = \text{BF}_4, \text{NO}_3, \text{ClO}_4$), each of which was crystallographically characterized. Electrocatalytic reduction of CO_2 was observed for each of the latter set of compounds.